

Chiral meson masses at the critical point from QCD in the improved ladder approximation

O. Kiriyaama*

Research Center for Nuclear Physics, Osaka University, Ibaraki 567-0047, Japan

Chiral meson masses at the critical point is investigated using QCD in the improved ladder approximation. We calculate the effective potential at finite temperature T and quark chemical potential μ and find the critical point at $T \simeq 95$ MeV, $\mu \simeq 290$ MeV. The chiral meson masses are determined from a second derivative of the effective potential at its minimum. We find that the sigma goes to massless at the critical point while pion remains massive. Our results are consistent with that of the linear sigma model in contrast to the Nambu–Jona-Lasinio model.

PACS: 11.10.Wx, 11.15.Tk, 11.30.Rd, 12.38.Lg

Recently there has been great interest in studying the phase structure of quantum chromodynamics (QCD). We expect that at sufficiently high temperature and/or density the QCD vacuum undergoes a phase transition into a chirally symmetric/deconfinement phase [1], a color superconducting phase [2]. They may be realized in high-energy heavy-ion collisions at the BNL Relativistic Heavy Ion Collider (RHIC) and CERN Large Hadron Collider (LHC). These phase transitions are also important in the physics of neutron (or quark) stars and the early universe.

In massless two-flavor QCD, as confirmed by using the lattice simulation [3] and several effective theories [4–10], the chiral phase transition at high temperature is probably second order. On the other hand, at high density a first order one is expected [4–10]. These observations indicate the existence of a tricritical point in the μ - T phase diagram for zero current quark masses and a critical point, where the first order transition ends, for nonzero current quark masses. The existence and the location of the critical point has been studied also by using the recently proposed lattice QCD method [11]. It is expected that the sigma field becomes massless at the critical point while the pion field remains massive and the critical point is in the same universality class as the three dimensional Ising model [12]. Recently, it has been proposed that this point may lead to characteristic signatures which enable us to explore the phase structure of QCD in heavy-ion collisions [13]. The behavior of the chiral meson masses around the critical point is studied within the framework of the linear sigma model and Nambu–Jona-Lasinio (NJL) model [5]. In the linear sigma model, the sigma mass goes to zero at the critical point. However, in the NJL model with the random phase approximation the sigma remains massive at the critical point. The chiral meson masses at finite temperature and density has been studied in another QCD motivated model [14], however, their behavior around the critical point has not been known yet. In this paper we investigate where the critical point locates and how the chiral meson masses behave around the critical point using the so-called *QCD in the improved ladder approximation* [7–10].

In the following we fix the scale parameter of our model by the condition $\Lambda_{QCD} = 1$ except for numerical calculations. Its value is determined by the condition $f_\pi = 93$ MeV at $T = \mu = 0$.

At zero temperature and zero chemical potential, the Cornwall-Jackiw-Tomboulis effective potential [15] for QCD in the improved ladder approximation is expressed as a functional of $\Sigma(p_E)$ and $\Sigma_5(p_E)$ [9], the scalar and the pseudo-scalar part of the dynamical mass function of the quark respectively

$$V = -2 \int \frac{d^4 p_E}{(2\pi)^4} \ln \frac{\Sigma^2(p_E) + \Sigma_5^2(p_E) + p_E^2}{p_E^2} - \frac{2}{3C_2} \int dp_E^2 \frac{1}{\Delta(p_E)} \left[\left(\frac{d}{dp_E^2} \Sigma(p_E) \right)^2 + \left(\frac{d}{dp_E^2} \Sigma_5(p_E) \right)^2 \right], \quad (1)$$

where the function

$$\Delta(p_E) = \frac{d}{dp_E^2} \frac{\bar{g}^2(p_E)}{p_E^2} \quad (2)$$

*E-mail: kiriyaama@rcnp.osaka-u.ac.jp

is introduced, p_E denotes the Euclidean momentum, $\bar{g}^2(p_E)$ is the QCD running coupling of one-loop order, C_2 is the quadratic Casimir operator for color $SU(N_c)$ group, and an overall factor (the number of light flavors times the number of colors) is omitted. Note that in the derivation of Eq. (1), the Higashijima–Miransky approximation [16,17] has been used and an infrared finite running coupling and quark mass functions like Eqs. (3), (4) and (5) are assumed. In this paper, we use the following effective running coupling [16]

$$\bar{g}^2(p_E) = \frac{2\pi^2 a}{\ln(p_E^2 + p_R^2)}, \quad (3)$$

where p_R is an infrared regularization parameter to keep the QCD running coupling from blowing up at $p_E = 1(\Lambda_{QCD})$, and $a = 8/9$ (we use three-flavor, three-color effective running coupling). Corresponding to the above running coupling, the Schwinger–Dyson equations, which are the extremum conditions of Eq. (1) with respect to $\Sigma(p_E)$ or $\Sigma_5(p_E)$, suggest the following trial mass functions

$$\Sigma(p_E) = m_R [\ln(p_E^2 + p_R^2)]^{-a/2} + \frac{\sigma}{p_E^2 + p_R^2} [\ln(p_E^2 + p_R^2)]^{a/2-1}, \quad (4)$$

$$\Sigma_5(p_E) = \frac{\sigma_5}{p_E^2 + p_R^2} [\ln(p_E^2 + p_R^2)]^{a/2-1}, \quad (5)$$

where σ (σ_5) is related to the renormalization group invariant (RGI) quark condensate $\langle \bar{q}q \rangle$ ($\langle \bar{q}i\gamma_5 q \rangle$) as $\sigma = 2\pi^2 a \langle \bar{q}q \rangle / 3$ ($\sigma_5 = 2\pi^2 a \langle \bar{q}i\gamma_5 q \rangle / 3$) and m_R is the RGI current quark mass. The explicit chiral symmetry breaking term is introduced in $\Sigma(p_E)$ alone as it should be.

We now turn to discussions about the effective potential at finite temperature and density. In order to calculate the effective potential at finite temperature and density we apply the imaginary time formalism [19]

$$\int \frac{dp_4}{2\pi} f(p_4) \rightarrow T \sum_{n=-\infty}^{\infty} f(\omega_n + i\mu), \quad (6)$$

where $\omega_n = (2n+1)\pi T$ ($n = 0, \pm 1, \pm 2, \dots$) is the fermion Matsubara frequency and μ represents the quark chemical potential. In addition, we need to define the running coupling and the trial mass functions at finite temperature and density. For simplicity, we adopt the following functional form for $\mathcal{D}_{T,\mu}(p)$, $\Sigma_{T,\mu}(p)$, and $\Sigma_{5;T,\mu}(p)$ by replacing p_4 in $\mathcal{D}(p_E)$, $\Sigma(p_E)$, and $\Sigma_5(p_E)$ with ω_n :

$$\mathcal{D}_{T,\mu}(p) = \frac{2\pi^2 a}{\ln(\omega_n^2 + |\vec{p}|^2 + p_R^2)} \frac{1}{\omega_n^2 + |\vec{p}|^2}, \quad (7)$$

$$\begin{aligned} \Sigma_{T,\mu}(p) = & m_R [\ln(\omega_n^2 + |\vec{p}|^2 + p_R^2)]^{-a/2} \\ & + \frac{\sigma}{\omega_n^2 + |\vec{p}|^2 + p_R^2} [\ln(\omega_n^2 + |\vec{p}|^2 + p_R^2)]^{a/2-1}, \end{aligned} \quad (8)$$

$$\Sigma_{5;T,\mu}(p) = \frac{\sigma_5}{\omega_n^2 + |\vec{p}|^2 + p_R^2} [\ln(\omega_n^2 + |\vec{p}|^2 + p_R^2)]^{a/2-1}. \quad (9)$$

A few comments are in order.

In Eq. (7) we do not introduce the μ dependence in $\mathcal{D}_{T,\mu}(p)$. The gluon momentum squared is the most natural argument of the running coupling at zero temperature and density, in the light of the chiral Ward–Takahashi identity [20,21]. Then it is reasonable to assume that $\mathcal{D}_{T,\mu}(p)$ does not depend on the quark chemical potential. In addition, the screening mass is not included in Eq. (7). As concerns the mass functions, we use the same function as Eqs. (4) and (5) except that we replace p_4 with ω_n . The quark wave function does not suffer the renormalization in the Landau gauge for $T = \mu = 0$, while, the same does not hold for finite temperature and/or density. Furthermore, we neglect the T and/or μ dependent terms in the quark and gluon propagators that arise from the perturbative expansion.

Substituting Eqs. (7), (8) and (9) into (1) and considering the differentiation with respect to p_E^2 to be that with respect to $|\vec{p}|^2$, we can write down the effective potential $V(\sigma, \sigma_5; m_R)$ (see the Appendix of Ref. [9]).

In numerical calculations, since it was known that the temperature and chemical potential dependence of the quantities such as $\langle \bar{q}q \rangle$ and f_π are stable under the change of the infrared regularization parameter

[7]. Therefore, in the first place, we fix $\ln(p_R^2/\Lambda_{QCD}^2) = 0.1$ and determine the value of Λ_{QCD} by the condition $f_\pi = 93$ MeV at $T = \mu = 0$ and in the chiral limit; i.e., $m_R = 0$. In this case, the pion decay constant is approximately given by Pagels–Stoker formula [22]:

$$f_\pi^2 = 4N_c \int \frac{d^4 p_E}{(2\pi)^4} \frac{\Sigma(p_E)}{(\Sigma^2(p_E) + p_E^2)^2} \left(\Sigma(p_E) - \frac{p_E^2}{2} \frac{d\Sigma(p_E)}{dp_E^2} \right), \quad (10)$$

and we obtain $\Lambda_{QCD} = 738$ MeV. Secondly, we assume the light quarks (u and d) are degenerate in mass and take the current quark mass evaluated at the renormalization point $\kappa = 1$ GeV as $m_u(1\text{GeV}) = 7\text{MeV}$. Using the one-loop evolution formula, the RGI current quark mass m_R extracted from the above-mentioned value becomes $m_R = 7.6 \times 10^{-3} \Lambda_{QCD}$. A discussion of the effective potential and the chiral symmetry restoration at high temperature and/or density can be found in Ref. [9].

Figure 1 shows the phase diagram in the chiral limit in n_B - T plane. The baryon number density n_B is defined as $n_B = n_q/3 = -(1/3)\partial V/\partial\mu$ with V renormalized so that it has the correct free theory behavior at $\sigma = \sigma_5 = 0$. At $T = 0$, for example, there is a mixed phase that consists of massive quarks with $n_B^{(-)} = 1.5n_0$ and massless quarks with $n_B^{(+)} = 4.3n_0$ where $n_0 = 0.17\text{fm}^{-3}$ is normal nuclear matter density. The phase diagram for $m_u(1\text{GeV}) = 7\text{MeV}$ case is shown in Fig. 2. The critical point E where the first order phase transition ends is found at $\mu_E \simeq 290$ MeV, $T_E \simeq 95$ MeV;

$$\frac{\mu_E}{\mu_{crit}} \simeq 0.64, \quad \frac{T_E}{T_{cross}} \simeq 0.70, \quad (11)$$

where μ_{crit} is the critical chemical potential at $T = 0$, and T_{cross} is the temperature where M_σ is minimized and M_π starts to increase at $\mu = 0$. We have confirmed that by the finite current quark mass the critical point is moved from the tricritical point, which we have found in the previous paper [9], toward larger value of μ and smaller value of T .

The values of the chiral meson masses are defined by multiplying the second derivative by the appropriate factor f :

$$M_\sigma^2 = f \frac{\partial^2 V}{\partial \sigma^2} \Big|_{\min}, \quad M_\pi^2 = f \frac{\partial^2 V}{\partial \sigma_5^2} \Big|_{\min}. \quad (12)$$

Here, “min” at the end of the equations means that they are evaluated at the minimum of $V(\sigma, \sigma_5; m_R)$. In this paper, we do not examine the factor f ; rather, we fix $M_\pi(T = \mu = 0)$ to 140 MeV, then, $M_\sigma(T = \mu = 0)$ turns out to be 668 MeV. The μ dependence of M_σ and M_π at $T = T_E$ is shown in Fig. 3. We find that sigma *almost* goes to massless at the critical point, while pion remains massive. The chiral meson masses at $\mu = \mu_E$ show behavior similar to Fig. 3 as functions of T . These behavior is consistent with that obtained in the linear the sigma model [5].

In conclusions, we investigated the phase structure and the chiral meson masses at the critical point from QCD in the improved ladder approximation. Using the variational approach, we calculated the effective potential at finite temperature and chemical potential. In the chiral limit, we found the mixed phase that consists of a low density chirally broken phase and a high density chirally symmetric phase when T is sufficiently small. For explicit chiral symmetry breaking case, the critical point was found at $\mu_E \simeq 290$ MeV, $T_E \simeq 95$ MeV. The value of μ_E seems to be too large in light of the experiments at RHIC and LHC. By including strange quark mass, however, it would be reduced. The meson masses was obtained from the curvature at the minimum of the effective potential. We found that M_σ almost goes to zero at the critical point while M_π remains nonzero. The result is consistent with that obtained within the framework of the linear sigma model in the mean-field approximation [5]. We have also confirmed that $\langle \bar{q}q \rangle_P$ at the tricritical point behaves as

$$\langle \bar{q}q \rangle_P \sim m_R^{1/5}.$$

Our results can be understood by the Landau-Ginzburg effective potential and partly support the experimental signature proposed in Ref. [13].

Finally, some comments are in order. In this paper we did not take into account the screening of the gluon, that is to say, the Debye screening for the electric gluons. Furthermore, it has been shown that at finite temperature the wave function renormalization makes non-negligible contribution to the critical line and the behavior of the order parameter [10]. They may affect the precise location of the

critical point although the main feature of this work might not change. In any case, it is preferable to take into account the screening of the gluon, wave function renormalization and the effects of s quark in the future work.

ACKNOWLEDGMENTS

The author is grateful to M. Maruyama and F. Takagi for valuable discussions.

-
- [1] For general reviews see, for example, J. Cleymans, R. V. Gavai, and E. Suhonen, Phys. Rep. **130** (1986), 217; L. McLerran, Rev. Mod. Phys. **58** (1986), 1021.
 - [2] See, for example, K. Rajagopal and F. Wilczek, *The Condensed Matter Physics of QCD*, hep-ph/0011333.
 - [3] S. Ejiri, Nucl. Phys. B (Proc. Suppl.) **94** (2001), 19.
 - [4] T. Hatsuda and T. Kunihiro, Phys. Rep. **247** (1994), 221.
 - [5] O. Scavenius, Á. Mócsy, I. N. Mishustin, and D. H. Rishke, Phys. Rev. C **64** (2001), 045202.
 - [6] A. Barducci, R. Casalbuoni, S. De Curtis, R. Gatto, and G. Pettini, Phys. Rev. D **41** (1990), 1610; Phys. Lett. B **240** (1990), 429; Phys. Rev. D **46** (1992), 2203; A. Barducci, R. Casalbuoni, G. Pettini, and R. Gatto, Phys. Rev. D **49** (1994), 426; C. D. Roberts and S. Schmidt, Prog. Part. Nucl. Phys. **45S1** (2000), 1.
 - [7] Y. Taniguchi and Y. Yoshida, Phys. Rev. D **55** (1997), 2283.
 - [8] M. Harada and A. Shibata, Phys. Rev. D **59** (1998), 014010.
 - [9] O. Kiriya, M. Maruyama, and F. Takagi, Phys. Rev. D **62** (2000), 105008; *ibid.* **63** (2001), 116009.
 - [10] T. Ikeda, hep-ph/0107105.
 - [11] Z. Fodor and S. D. Katz, hep-ph/0104001; hep-lat/0106002; hep-lat/0111064.
 - [12] M. A. Halasz, A. D. Jackson, R. E. Shrock, M. A. Stephanov, and J. J. M. Verbaarschot, Phys. Rev. D **58** (1998), 096007; J. Berges and K. Rajagopal, Nucl. Phys. **B538** (1999), 215.
 - [13] M. Stephanov, K. Rajagopal, and E. Shuryak, Phys. Rev. D **60** (1999), 114028; B. Berdnikov and K. Rajagopal, Phys. Rev. D **61** (2000), 105017; K. Rajagopal, Acta Phys. Polon. B **31** (2000), 3021.
 - [14] A. Barducci, R. Casalbuoni, G. Pettini, and R. Gatto, Phys. Rev. D **63** (2001), 074002.
 - [15] J. M. Cornwall, R. Jackiw, and E. Tomboulis, Phys. Rev. D **10** (1974), 2428.
 - [16] K. Higashijima, Phys. Lett. B **124** (1983), 257; Phys. Rev. D **29** (1984), 1228; Prog. Theor. Phys. Suppl. **104** (1991), 1.
 - [17] V. A. Miransky, Yad. Fiz. **38** (1983), 468 [Sov. J. Nucl. Phys. **38** (1983), 280].
 - [18] K-I. Aoki, M. Bando, T. Kugo, M. G. Mitchard, and H. Nakatani, Prog. Theor. Phys. **84** (1990), 683.
 - [19] See, for example, J. I. Kapusta, *Finite Temperature Field Theory* (Cambridge University Press, Cambridge, England, 1989).
 - [20] P. Jain and H. J. Munczek, Phys. Rev. D **44** (1991), 1873.
 - [21] T. Kugo and M. G. Mitchard, Phys. Lett. B **282** (1992), 162; *ibid.* **286** (1992), 355.
 - [22] H. Pagels and S. Stoker, Phys. Rev. D **20** (1979), 2947.

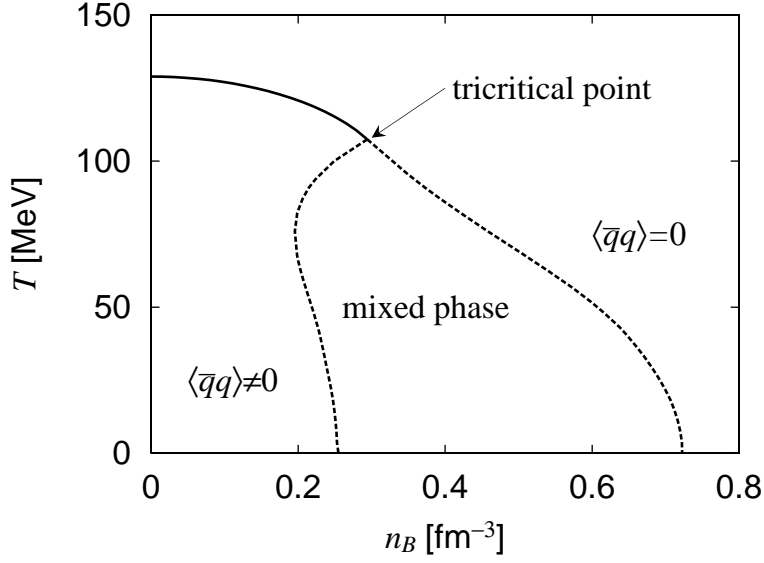


FIG. 1. The phase diagram in the chiral limit as a function of the baryon density and the temperature. The solid line indicates the phase transition of second order and the dashed lines indicate that of first order.

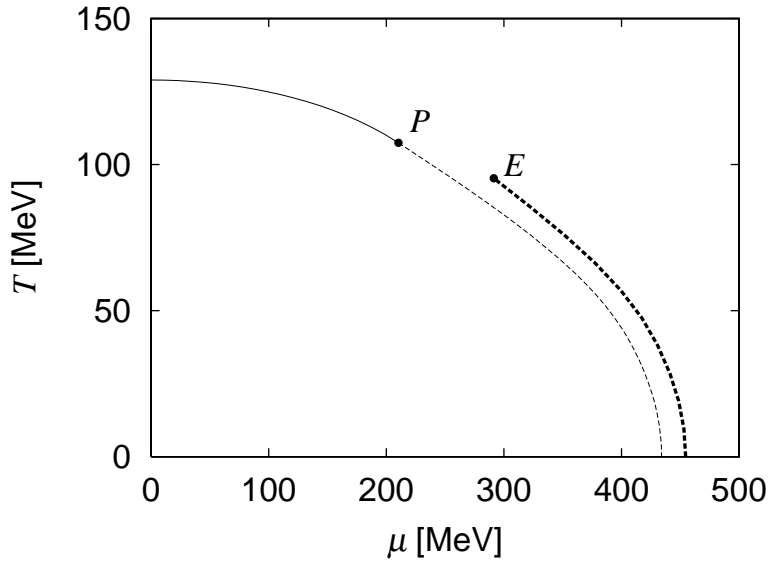


FIG. 2. The phase diagram in μ - T plane. The solid line indicates the phase transition of second order and the dashed line indicates that of first order. The thin line corresponds to the chiral limit and the thick line corresponds to $m_R(1\text{GeV}) = 7\text{MeV}$ case. The points P and E represent the tricritical point and the critical point, respectively. We note that the critical chemical potential at $T = 0$ is slightly (about 2%) larger than previous papers [9] because we have improved the numerical calculation.

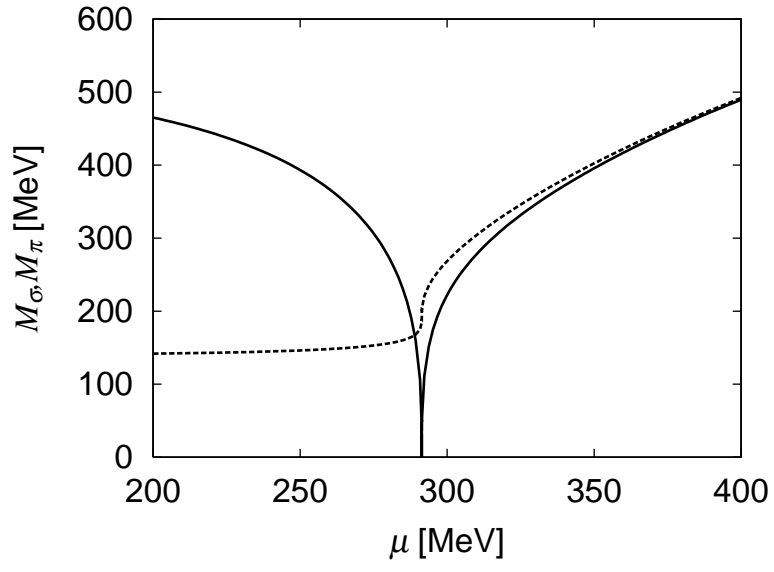


FIG. 3. The chemical potential dependence of M_σ (solid line) and M_π (dotted line) at $T = T_E$.